

AperTO - Archivio Istituzionale Open Access dell'Università di Torino

Anodic microbial community analysis of microbial fuel cells based on enriched inoculum from freshwater sediment.

This is the author's manuscript

Original Citation:

Availability:

This version is available <http://hdl.handle.net/2318/1689009> since 2019-02-01T09:57:27Z

Published version:

DOI:10.1007/s00449-019-02074-0

Terms of use:

Open Access

Anyone can freely access the full text of works made available as "Open Access". Works made available under a Creative Commons license can be used according to the terms and conditions of said license. Use of all other works requires consent of the right holder (author or publisher) if not exempted from copyright protection by the applicable law.

(Article begins on next page)



Anodic microbial community analysis of microbial fuel cells based on enriched inoculum from freshwater sediment

Journal:	<i>Bioprocess and Biosystems Engineering</i>
Manuscript ID	BPBSE-18-0255.R1
Type of Manuscript:	Research Paper
Date Submitted by the Author:	07-Dec-2018
Complete List of Authors:	<p>Armato, Caterina; University of Torino, Department of Public Health and Pediatrics; Istituto Italiano di Tecnologia, Centre for Sustainable Future Technologies (CSFT@PoliTo)</p> <p>Ahmed, Daniyal; Istituto Italiano di Tecnologia, Centre for Sustainable Future Technologies (CSFT@PoliTo); Politecnico di Torino, Department of Applied Science and Technology</p> <p>Agostino, Valeria; Istituto Italiano di Tecnologia, Centre for Sustainable Future Technologies (CSFT@PoliTo); Politecnico di Torino, Department of Applied Science and Technology</p> <p>Traversi, Deborah; University of Torino, Department of Public Health and Pediatrics</p> <p>Degan, Raffaella; University of Torino, Department of Public Health and Pediatrics</p> <p>Tommasi, Tonia; Politecnico di Torino, Department of Applied Science and Technology</p> <p>Margaria, Valentina; Istituto Italiano di Tecnologia, Centre for Sustainable Future Technologies (CSFT@PoliTo)</p> <p>Sacco, Adriano; Istituto Italiano di Tecnologia, Centre for Sustainable Future Technologies (CSFT@PoliTo)</p> <p>Gilli, Giorgio; University of Torino, Department of Public Health and Pediatrics</p> <p>Quaglio, Marzia; Istituto Italiano di Tecnologia, Centre for Sustainable Future Technologies (CSFT@PoliTo)</p> <p>Saracco, Guido; Istituto Italiano di Tecnologia, Centre for Sustainable Future Technologies (CSFT@PoliTo)</p> <p>Schilirò, Tiziana; University of Torino, Department of Public Health and Pediatrics</p>
Keywords:	Freshwater sediment, microbial communities, DGGE, real time qPCR, MFC

1 Anodic microbial community analysis of microbial fuel cells based on enriched
2 inoculum from freshwater sediment

3 Caterina Armato^{a,b}, Daniyal Ahmed^{b,c}, Valeria Agostino^{b,c}, Deborah Traversi^a, Raffaella
4 Degan^a, Tonia Tommasi^c, Valentina Margaria^b, Adriano Sacco^b, Giorgio Gilli^a, Marzia
5 Quaglio^b, Guido Saracco^b, Tiziana Schiliro^{a*}

6
7 ^a*Department of Public Health and Pediatrics, University of Torino, Torino, Italy;*
8 ^b*Centre for Sustainable Future Technologies (CSFT@PoliTo), Istituto Italiano di*
9 *Tecnologia, Torino, Italy;*
10 ^c*Department of Applied Science and Technology, Politecnico di Torino, Torino, Italy.*

11
12
13 ^{*}*Department of Public Health and Pediatrics, University of Torino, Piazza Polonia 94,*
14 *10126 Torino, Italy*
15 *e-mail: tiziana.schiliro@unito.it*
16 *telephone: +390116705820*
17 *fax numbers: +390116705874*

Abstract

The characterization of anodic microbial communities is of great importance in the study of microbial fuel cells (MFCs). These kinds of devices mainly require a high abundance of anode respiring bacteria (ARB) in the anode chamber for optimal performance. This study evaluated the effect of different enrichments of environmental freshwater sediment samples used as inocula on microbial community structures in MFCs. Two enrichment media were compared: ferric citrate (FeC) enrichment, with the purpose of increasing the ARB percentage, and general enrichment (Gen). The microbial community dynamics were evaluated by polymerase chain reaction denaturing gradient gel electrophoresis (PCR-DGGE) and real time polymerase chain reaction (qPCR). The enrichment effect was visible on the microbial community composition both during precultures and in anode MFCs. Both enrichment approaches affected microbial communities. Shannon diversity as well as β -Proteobacteria and γ -Proteobacteria percentages decreased during the enrichment steps, especially for FeC ($p < 0.01$). Our data suggest that FeC enrichment excessively reduced the diversity of the anode community, rather than promoting the proliferation of ARB, causing a condition that did not produce advantages in terms of system performance.

Keywords: Freshwater sediment; microbial communities; DGGE; real time qPCR; MFC.

Introduction

A biological approach to the study of microbial electrochemical technologies (METs) can increase knowledge within the microbial electrochemistry field. The need for a better understanding of anodic microbial community composition is of great importance in studying microbial electrochemical cells, including microbial fuel cells (MFCs). MFCs are biocatalyzed systems able to convert chemical energy into electrical energy using anaerobic respiration by electroactive microorganisms known as anode respiring bacteria (ARB) [1, 2]. Typically, they consist of two compartments separated by a proton exchange membrane (PEM) with an external circuit connecting anode and cathode electrodes. In these devices, the anode biofilm acts as a biocatalyst to hydrolyse the substrate and release protons and electrons in MFCs; therefore, the higher the amount of ARB in the anodic biofilm, the higher the electrical energy production [3]. In MFCs, the anode acts as a terminal electron acceptor in the same manner as any other natural acceptor, e.g. oxygen, nitrate or Fe(III) [4, 5].

It is known that electrochemically active microorganisms can interface with the electrode in several ways [6], although exoelectrogenic mechanisms in microbial species are still an open field of research, and many different new microbial strains show extracellular electron transfer capacities [7]. ARB can be found and enriched from many different environmental sources, such as freshwater and marine sediments, salt marshes, anaerobic sludge, industrial effluent and sludge from wastewater treatment plants [1, 5, 8, 9]. The microbial community composition is affected by the inoculum source and the type of enrichment as well as by the more thoroughly investigated system design and operating parameters [3].

Different approaches have been reported in the literature to optimize the formation of a high performing anode microbial community [10, 11]. However, most of them are based on the use of already formed biofilm, or other elements of pre-existing bioelectrochemical systems [12–14]. On the contrary, enrichment procedures directly acting on the inoculum represent a more efficient approach [5].

Considering the substantial agreement on the pivotal role of ARB in MFC microbial community, it has been proposed to promote their specific selection by means of iron enrichment methods [5, 15]. To this aim, it is possible to use ferric citrate (FeC), which selects for microorganisms that are able to reduce Fe(III); meanwhile, other bacteria without the required ability are eliminated, consequently increasing the percentage of electrochemically active bacteria [8]. Pierra et al. [5] evaluated the use of an iron enrichment method to target dissimilatory metal-reducing bacteria. Sathish-Kumar et al. [15] compared an Fe(III) enrichment method against an electrochemical procedure as well as a combination of the two. According to literature, enrichment with Fe(III) citrate allowed the selection of ARB to mimic the role of a MFC carbon electrode working as an electron acceptor [6, 15, 16].

Different opinions are reported in literature about the correlation between microbial diversity and the performance of MFCs. Torres et al. showed that the lower-diversity type of MFC exhibits higher performance [17], but some years later, Stratford et al. obtained a strong correlation in a regression model between the power output of the system and the Shannon index, which was then proposed as a predictor of good performances [18].

Yamamoto et al. pointed out the relevance of the analysis of both the planktonic and attached components; in his study, he showed that the correlation between biofilm and planktonic microbes was important to achieve better performance [19].

In the present study, experiments were designed to find the reason why the performance of Fe(III)-type MFC was lower than the control MFC.

In line with this, we investigated the impact of freshwater sediment enrichments on the structure and composition of microbial community sampled from planktonic component, carbon felt biofilm and graphite rod biofilm.

The effect of a Fe(III) enrichment procedure was compared with a general (non-specific) enrichment. Electrochemical performance and biofilm morphology were previously evaluated in Agostino et al. [20]. A combination of denaturing gradient gel electrophoresis (DGGE), a community structure technique and real time quantitative polymerase chain reaction (qPCR), a population technique [21] was applied to investigate the changes in and the diversity of the microbial community.

This work represents the first attempt to describe the effect of ferric citrate enrichment on a microbial community in a MFC system from a biomolecular point of view.

Materials and Methods

Experimental set up

A freshwater sediment sample (Bagnère Creek, Valle D'Aosta, Italy) was enriched under anaerobic conditions with two different media: a Ferric Citrate (FeC) medium and a General (Gen) medium. Sodium acetate was used as an electron donor and carbon source in both enrichment methods; media composition and operational protocol were as previously reported [20]. Briefly, the composition of FeC medium was the following: Fe(III) citrate 13.70 g/L; NaHCO₃ 2.50 g/L; NH₄Cl 1.50 g/L; NaH₂PO₄ 0.60 g/L; KCl 0.10 g/L; Na acetate 2.50 g/L; Wolfe's Vitamin solution 10 mL/L (ATCC) and Wolfe's trace mineral solution 10 mL/L (ATCC). The composition of the Gen medium was the following: NH₄Cl 1.50 g/L; NaH₂PO₄ 2.45 g/L; Na₂HPO₄ 4.28 g/L; KCl 0.10 g/L; Na acetate 2.50 g/L; Wolfe's Vitamin solution 10 mL/L (ATCC) and Wolfe's trace mineral solution 10 mL/L (ATCC).

The microbial cultures were subjected to three sequential enrichments for 21 days of total growth at room temperature (21 ± 2 °C) and with gentle orbital shaking (150 rpm). They were then inoculated into the two-chamber MFCs, with a ratio of 10% v/v of the total anode volume. At each step, 10% (v/v) of the microbial cultures were inoculated in fresh anaerobic media. Before inoculation, the media were purged by high-speed N₂ flow for 15 minutes in order to reach anaerobic conditions. Biofilm formation into the anodic chamber was carried out by applying a low external resistance (47 Ω), resulting in a positive anode potential polarization.

MFCs operated in continuous mode with a hydraulic retention time of 5 days (0.5 mL/h). The anolyte consisted of 1 g/L per day of CH_3COONa and 0.31 g/L per day of NH_4Cl dissolved into a phosphate buffer solution (PBS: NaH_2PO_4 2.45 g/L; Na_2HPO_4 4.28 g/L; KCl 0.10 g/L) with 10 mL/L of Wolfe's vitamin solution (ATCC) and 10.00 mL/L Wolfe's trace mineral solution (ATCC). The catholyte was comprised of 6.58 g/L $\text{K}_3[\text{Fe}(\text{CN})_6]$ dissolved into PBS.

Carbon felt (Soft felt SIGRATHERM GFA5, SGL Carbon, Germany) was used as the material for anode and cathode electrodes. A cation exchange membrane (CEM, CMI-7000, Membranes International Inc., USA) was used to separate the two compartments. Electrical contacts to the electrodes were made using graphite rods.

The experiments were performed in duplicate, at room temperature conditions (20-22°C), and lasted 90 days.

A data acquisition system (Agilent 34972A) was used to monitor cell voltage continuously across the external resistor and anodic potentials.

Electrochemical characterization and bioanode imaging analysis were performed as previously reported [20] to evaluate the performances of the devices. Polarization curves were obtained at the end of the biofilm acclimation phase during changing external circuit resistances. Anode impedance spectra were recorded using a multi-channel VSP potentiostat in a 3-electrode configuration for each polarization condition. Cyclic voltammetry (CV) was performed using the same potentiostat to obtain the putative electron transfer redox centre. Bioanode imaging was acquired by fluorescent microscopy to characterize the biofilm distribution within the electrode after LIVE/DEAD staining.

DNA extraction

Carbon felt biofilm and graphite rod samples were subjected to a pre-treatment; 1.25 g each of wet anode electrode and graphite rods were washed twice with 4 mL of 0.9% NaCl. Supernatants were centrifuged for 20 min at 10000 rpm. Pellets were re-suspended in 0.9% of NaCl solution. DNA was extracted from each sample using a commercial kit (UltraClean™ Microbial DNA Isolation Kit, MO-BIO Laboratories, Inc., Carlsbad, CA), following manufacturing information. Genomic DNA integrity was checked by electrophoresis gel on a 2% agarose gel and 1X TBE (Tris-Borate-EDTA) buffer after each extraction as previously described [22].

The quantification of the extracted DNA was performed by fluorometric quantification using a Qubit™ Fluorometer and a Qubit™ dsDNA HS Assay by Invitrogen (Life Technology, Ltd., Paisley, UK) according to manufacturer instructions.

PCR-DGGE and Sequencing

Primer 357F with GC clamp and 518R were used to amplify the V3 region of the 16S rRNA genes from the bacterial community [23]. The PCR amplification was performed in a 50-μl volume containing 0.2 μM of each primer, 0.2 mg/ml of Bovine Serum Albumin (BSA) and 1X of Master Mix for PCR (Bio-Rad).

PCR was performed in T100 thermal cycler (Bio-Rad, Italy) as follows: ten cycles of denaturation at 94 °C for 30 s, annealing at 55 °C for 30 s and extension at 72 °C for 1 min; twenty-five cycles of denaturation at 92 °C for 30 s, annealing at 52 °C for 30 s and extension at 72 °C for 1 min; followed by a single final extension at 72 °C for 10 min.

The PCR products were approximately 190 bp in length. DGGE was carried out using the DCode™ Universal Detection System (Bio-Rad Laboratories, CA, USA) as previously described by Webster et al. [24]. Ten microliters of the PCR product were loaded onto 8% polyacrylamide gels (acrylamide: bis-acrylamide, 37.5:1) with denaturing gradients ranging from 30% to 50% (where 100% denaturant contains 7 mol L⁻¹ urea and 40% formamide) in 1X TAE buffer. The electrophoresis was run at a constant voltage of 200 V at 60 °C for 5 h. After that, the gel was stained with SYBR® Green I nucleic acid gel stain (Sigma-Aldrich), visualized on a UV transilluminator and photographed (Gel Doc XR+ System, Bio-Rad). The computerized images of DGGE profiles were analysed with the Quantity One software, Version 4.6.7 (Bio-Rad Laboratories, CA, USA).

DGGE bands recurrent at the site level, or shared among different sites, were excised and rinsed in 50 μL of deionized water. The gel bands were then crushed in 10 μL of sterile mmQ water and stored at -20 °C. DNA extracts from excised DGGE bands were used as templates and PCR was performed as described above, except for the elimination of BSA and the employment of modified bacterial reverse primers (357F-GC-M13R and 518R-AT-M13F), as previously described [25]. PCR products were sent to the Genechron (Ylichron S.R.L.) laboratory for Sanger sequencing. The sequences were then compared with the NCBI database using nucleotide Basic Local Alignment Search Tool (BLASTn) analysis (<http://www.ncbi.gov/>).

Real time qPCR

DNA was also used for qPCR absolute quantification assays. Specific primers targeting different bacterial phyla and classes were selected from the scientific literature based on sequence analysis (Table 1). Moreover, we selected primers to detect typically electroactive microorganisms such as *Geobacteriaceae* and *Pseudomonas* spp.

The qPCR reactions targeting specific regions of 16S rRNA were performed with SYBR® Green chemistry in 20 µL total volume of SsoAdvanced™ Universal SYBR® Green Supermix (Bio-Rad, Italy) 1X, 2 µL of 1:10 DNA as template and 250 nM of each primer. Total bacteria were quantified with TaqMan® chemistry in 20 µL total volume of iQ™ Multiplex Powermix (Bio-Rad, Italy) 1X, 2 µL of 1:10 DNA as template, 250 nM of each primer and 100 nM of probe. Each reaction was performed in triplicate with a CFX96 Touch™ Real-Time PCR Detection System (Bio-Rad, Italy). The bacterial concentration from each sample was calculated by comparing the threshold cycle values obtained from the standard curves using the CFX Manager™ software. Standard curves for absolute quantifications were constructed using 10-fold serial dilutions of specific standard genomics (Table 1); the number of bacteria was expressed in terms of the number of gene copies, which is comparable between different samples.

The different strains used were obtained from ATCC (*Alcaligenes faecalis* ATCC® 8750D-5™, *Bacteroides fragilis* ATCC® 25285D-5™, *Clostridium difficile* ATCC® 9689D-5™, *Desulfovibrio vulgaris* ATCC® 29579D-5™, *Geobacter metallireducens* ATCC® 53774D-5™, *Pseudomonas aeruginosa* ATCC® 15442™).

Negative controls containing all of the elements of the reaction mixture except template DNA were performed in every analysis and no product was ever detected. The amplification efficiency of the qPCR for all primer pairs was determined using the linear regression slope of a dilution series.

Reaction protocols are reported in Table 2. Melt curve analysis was performed at the end of each amplification reaction, with the exception of total bacteria, by slowly heating the qPCR products from 65 °C to 95 °C, in increments of 0.5 °C for 5 seconds with simultaneous measurement of the SYBR Green signal intensity. Melting-point-determination analysis allowed the confirmation of the specificity of the amplification products. All qPCRs were considered valid if they had linear standard curves with an $R^2 > 0.980$ and an efficiency between 90 and 105% (Bio-Rad, Real-Time PCR Applications Guide).

Data analysis and statistics

The DGGE profiles were compared using cluster analysis (BioNumerics software, version 7.6, Applied Maths, Ghent, Belgium) using band-based similarity coefficients (i.e. Jaccard coefficients) for the construction of similarity matrices and the UPGMA algorithm was used to obtain the dendrograms [33–37].

The Shannon index was calculated using BioNumerics software version 7.6 (Applied Maths, Ghent, Belgium). Absolute and relative quantifications were calculated using the qPCR data.

Student's t-tests and one-way ANOVAs with a Tukey's post hoc analysis were performed to compare two or more groups of independent samples.

For the Student's t-test, variance homogeneity was first assessed using the Levene's test; thus, an equal variance for Tukey's test was assumed for multiple post hoc comparisons. The differences between means were considered significant at $p < 0.05$. Statistical analysis was performed using SPSS software (version 24.0 for Windows).

Results and Discussion

Freshwater sediment samples were anaerobically enriched with two different media, with and without Fe(III)citrate in order to evaluate the effect of enrichment on the microbial community that developed in the anode chamber of the MFCs. Each third sequential enrichment was then inoculated into the MFCs and acclimatized.

Enrichment effect on precultures

The effect of both kinds of enrichment (i.e. FeC or Gen) on the freshwater sediment was already detectable after the first preculture step. DGGE analysis showed all enrichment steps differed considerably from the freshwater sediment sample (Jaccard similarity = 28.0%). The similarity between the Gen enrichment precultures was higher than between the FeC ones (Jaccard similarity = 76.9% and 52.9%, respectively) (Figure 1a). The presence of an anaerobic environment and FeC in the medium affected the diversity of the microbial community; the Shannon diversity index decreased during the enrichment steps, especially in the third FeC preculture (ANOVA, Tukey's post hoc: $p < 0.001$) (Figure 1b). This can be interpreted as a marker of the effect of the specific enrichment on the microbial

community. In fact, Shannon diversity indexes provide information about richness (the number of present species) and evenness (how abundances are distributed across species), and was proved to be positively correlated with power output [18].

Sequencing analysis revealed that, in our samples, the majority of bacteria belonged to the Proteobacteria and Firmicutes phyla (Table 3). Microorganisms belonging to β -Proteobacteria, γ -Proteobacteria, ϵ -Proteobacteria, δ -Proteobacteria and Bacilli classes dominated our community, which was in line with previous literature [8, 38].

Many uncultured bacteria such as *Comamonas* spp., *Dysgonomonas* spp., *Acrobacter* spp., *Alcaligenes* spp. and *Citrobacter* spp. were also detected, probably because of the environmental origin of the inoculum [39].

Coherently with the sequencing, quantitative analysis of the main microbial components revealed that the inoculum was mainly comprised of β -Proteobacteria (36.1%) and γ -Proteobacteria (41.0%) (Figure 2).

Their percentages decreased during enrichment steps, especially in the third FeC enrichment steps (β -Proteobacteria, < 1% and γ -Proteobacteria, 3.6%), confirming that the more selective FeC enrichment method has a major effect on the equilibrium of the microbial community when compared to the Gen enrichment method [20]. β -Proteobacteria subclasses consist of several groups of aerobic or facultative bacteria, which are often highly versatile in their degradation capacities [40]. Decrease in their relative quantities during the enrichment steps was possibly due to an anaerobic environment during precultures.

The microbial community at the third Gen enrichment step resulted in a population more dominated by Proteobacteria (beta, gamma and delta classes) and Bacteroidetes phyla as compared to the first FeC step (22% and 3% vs 4% and 1%, respectively). Only the Firmicutes phylum had higher percentage at the third FeC enrichment step than at the Gen steps (1% vs 0.3%, respectively) (Figure 2). Electrochemically active microorganisms, such as *Geobacteriaceae* spp. and *Pseudomonas* spp., decreased more in FeC enrichments than in general ones (Figure 3). FeC enrichment steps negatively affected *Geobacteriaceae* spp. (ANOVA, Tukey's post hoc: $p < 0.001$). On the contrary, they did not differ between the inoculum and third Gen enrichment step (ANOVA, Tukey's post hoc: $p > 0.05$). *Pseudomonas* spp. decreased at a statistically significant rate throughout the steps of both Gen and FeC enrichment (ANOVA, Tukey's post hoc: $p < 0.01$), especially in FeC enrichment.

The lower diversity and presence of these microorganisms, both in absolute and relative quantification, in the third FeC enrichment step as compared to the Gen steps explains the performance of the devices

inoculated by Gen enriched preculture: Gen-MFCs exhibited higher current and power density than FeC-MFC ones ($74 \pm 4 \text{ mA/m}^2$ vs $50 \pm 3 \text{ mA/m}^2$; $79 \pm 12 \text{ mW/m}^2$ vs $38 \pm 2 \text{ mW/m}^2$, respectively) and shorter start-up time (5 days vs 10 days, respectively) (data shown in [20]). Although previous studies showed that the FeC enrichment improved MFCs' performance [5, 15], this could be dependent on its concentration. Of note, in a recent work by Liu et al., [41] optimal community development was obtained at a Fe(III) concentration much lower than the one used in the present research.

Enrichment effect on MFC communities

As observed for the preculture steps, FeC enrichment also affected the microbial community developed in MFCs anodes. Biological analyses performed on the MFCs anodic compartments revealed that the kind of enrichment is the main source of diversity (similarity 48.7%) (Figure 4a). Even though qPCR showed no differences between Gen-MFCs and FeC-MFCs for all types of strains researched (t-test, $p > 0.05$), Shannon diversity was higher in the Gen-MFCs when compared with those of FeC-MFCs (t-test, $p < 0.05$) (Figure 4b). As observed during the early steps of the test, and until the end of the start-up time, the Shannon diversity, which was strongly associated with power [18], could explain the better performance of Gen-MFCs. Three-electrode EIS analysis suggested a more efficient electron transfer mechanism in the Gen-MFCs' bioanodes as opposed to the FeC-MFCs' bioanodes. By this impedance analysis, it is possible to recognize two features: a high-frequency process, which is related to the electron charge transfer (activation resistance) and a low frequency process, accounting for the anodic biofilm mass-transfer limitation (diffusion resistance), mainly dependent upon the diffusion of the organic substrate in the biofilm. Gen-MFCs bioanode, with its higher Shannon diversity and more dense and active mixed consortia, is associated to a higher consumption rate of substrate, that decreases diffusion resistance, and hence accelerates electrons-transfer mechanisms, with respect to FeC-MFCs, where the diffusion time constant is about 4 times lower than Gen-MFCs. This resistance strongly depends on the applied external resistances, which are higher at open circuit voltage conditions and lower at the maximum power point. Moreover, the presence of a higher percentage of dead/inactive bacteria covering the interface between the bulk solution and the anodic electrode of FeC-MFCs, which was detected by Fluorescence Microscopy (Agostino et al., [20]) contributed to an increase in the resistance related to the interfacial process, i.e. double layer capacitance.

279 DGGE analysis showed higher similarity between the anode suspension and the carbon felt biofilm, as
 280 shown by the dendrogram in Figure 4a. Jaccard similarity of 92.3% and 84.6% was found for suspension
 281 and carbon felt biofilm of Fe-MFCs and Gen-MFCs, respectively. This is, to some extent, an
 282 unanticipated result, since higher similarity between the carbon felt biofilm and the graphite rod biofilm
 283 might be expected. In fact, graphite rod and anode carbon felt are constantly in contact. This unexpected
 284 result could be due to the carbon felt properties. Indeed, it is a porous material, and during the
 285 experiment, it was soaked in the anode medium. Thus, at the moment of the analysis, it also contained
 286 suspension, which could have led to high similarity between bacteria communities of anode biofilm and
 287 planktonic component.
 288 Real time qPCR analysis at the end of the MFCs' operation suggested that the community was dominated
 289 by β -Proteobacteria both in planktonic samples and the attached component (i.e. carbon felt biofilm and
 290 graphite rod biofilm) of all MFCs (Gen-MFCs: 26.13% and 24.42%; FeC-MFCs: 44.45% and 37.06%,
 291 respectively) (Figure 5). β -Proteobacteria in the planktonic component was statistically significantly
 292 higher in the FeC-MFCs than in Gen-MFCs (ANOVA: Tukey's post hoc, $p < 0.05$). These data confirmed
 293 the outcome of the sequencing analysis (Table 4). β -Proteobacteria was found to be the most abundant
 294 class within the Proteobacteria phylum in numerous previous studies using two-chamber MFCs, with
 295 different inocula and a variety of substrates, like synthetic wastewater or a liquid fraction of pig slurry
 296 (see for example [42, 43]).
 297 Interestingly, δ -Proteobacteria percentage increased from the inoculum (2.17%) to the end of the
 298 experiment (Gen-MFCs: 22.36% and 22.78%; FeC-MFCs: 22.85% and 15.87% in planktonic and
 299 attached components, respectively). Moreover, their percentage was doubled on the carbon felt biofilms
 300 compared to the graphite rod biofilms of Gen-MFCs (24.19% vs 12.99%). On the other hand, the reverse
 301 condition was found for FeC-MFCs (15.23% vs 31.35%). As in Chae et al. [40], δ -Proteobacteria were the
 302 second most frequently detected bacteria class in MFCs. The δ -Proteobacteria class, including
 303 *Geobacteraceae* spp., was found to be statistically significantly higher in the attached component of Gen-
 304 MFCs than in the FeC ones (ANOVA: Tukey's post hoc, $p < 0.05$).
 305 Differently from δ -Proteobacteria, the percentage of γ -Proteobacteria, which are largely facultative
 306 anaerobes [7], decreased from inoculum (40.96%) to end of the experiment (Gen-MFCs: 17.98% and
 307 14.28%; FeC-MFCs: 17.28% and 9.90% in planktonic and attached component, respectively). The γ -
 308 Proteobacteria class was found in statistically significantly higher amounts in the attached component of

Gen-MFCs (ANOVA: Tukey's post hoc, $p < 0.05$). Bacteroidetes were found to be statistically significantly higher in all components of Gen-MFCs (ANOVA: Tukey's post hoc, $p < 0.05$), although their percentages were quite similar in both Gen and FeC-MFCs, ranging between 1.79 and 2.53%. Bacteria in the Firmicutes phylum, which contains both obligate anaerobes (such as *Clostridia* spp.) and facultative anaerobes (such as *Bacilli* spp.) [7] was a smaller component in the MFCs, as they already were in the inoculum. Their percentage was always less than 0.1%. Firmicutes quantification indicated their higher presence in the attached component instead of in the suspension of both types of MFCs (ANOVA: Tukey's post hoc, $p < 0.05$); their presence was also higher in the FeC-MFCs attached components than in Gen ones (ANOVA: Tukey's post hoc, $p < 0.05$).

Along with Proteobacteria, Firmicutes is often among the predominant phyla composing the anode biofilm, regardless of configuration, inoculum or substrate [38, 42, 44, 45]. However, qPCR detected it in low percentages in each step of our analysis, for either FeC or Gen enrichment. This result could depend on the specific freshwater inoculum used for our work. As was pointed out by Hu et al. [46], Firmicutes seem to be more characteristic of planktonic samples, rather than sediments, as it was the case of the present study. Real time data confirmed the high similarity between suspension and carbon felt biofilms for both Gen-MFCs and Fe-MFCs; the Gen planktonic component was statistically similar to Gen biofilm for all kinds of strains with the exception of *Geobacteriaceae* and *Pseudomonas* spp., which were higher in the biofilm (ANOVA: Tukey's post hoc, $p < 0.001$) [7, 47], as well as higher in their relative percentage. Similar behaviour is shown by FeC-MFCs; the planktonic component that differs from carbon felt biofilm only for the large number of total bacteria and *Geobacteriaceae* spp. in the biofilm (ANOVA: Tukey's post hoc, $p < 0.001$).

In comparing the attached components in the MFCs, we can confirm that, from CV analysis (data shown in [20]), *Geobacteriaceae* spp. had the main role in the electron transfer in Gen-MFCs (midpoint potential equal to -0.4 V vs Ag/AgCl) and *Pseudomonas* spp. had the main role in FeC-MFCs (midpoint potential equal to -0.215 V). Real time quantification showed *Geobacteriaceae* spp. higher in Gen-MFCs than in FeC-MFCs and *Pseudomonas* spp. higher in FeC-MFCs than in Gen MFCs, even if there was not a statistically significant difference (ANOVA: Tukey's post hoc, $p > 0.05$). The lack of significant variation within the data of that comparison could be explained by the presence of a higher number of dead microorganisms in the FeC anode biofilms according to quantification. Indeed, qPCR quantifies both living and dead microorganisms; therefore, we had to take in to account the morphological

1
2
3 339 characterization of the anode microbial biofilm by fluorescence microscopy; the ratio between living and
4
5 340 dead microorganisms was higher in Gen-enriched bioanodes than in FeC-enriched ones (2.9 ± 0.5 and 1.4
6
7 341 ± 0.4 , respectively) [20].
8

9 342

10
11 343 **Conclusion**

12
13 344 Combined use of DGGE and qPCR biological approaches to study the microbial community growing in
14
15 345 anode chambers allowed us to characterize 86% of the freshwater sample and between 64% - 87% of the
16
17 346 anode community. This is a higher percentage than found from previous studies [22, 48] and is in line
18
19 347 with the results from other biological approaches in MFC investigation [49–51]. The qPCR confirmed
20
21 348 sequencing analysis performed on the bands cut from the DGGE gels. This approach proved to be useful
22
23 349 to have a quite full and detailed understanding of the dynamic evolution of the anodic microbial
24
25 350 communities, without high costs in terms of budget and time [21, 52–54].
26
27 351 Pre-enrichment steps with FeC strongly affected the equilibrium of the microbial community. However,
28
29 352 rather than facilitating the growing of ARB, which were thought to be the most responsible for current
30
31 353 production, the procedure just generally reduced the population diversity. On the contrary, the MFCs
32
33 354 exposed to Gen enrichment showed a more heterogeneous community and had a better performance than
34
35 355 the FeC ones. Our findings suggest that the use of a highly selective method of enrichment seems to be
36
37 356 detrimental to the formation of an anode microbial community adequate for operating inside MFCs.
38

39 357 **Declaration of interest**

40
41 358 The authors declare no conflict of interest.
42

43 359

44
45 360

46
47 361

48
49 362

50
51 363

52
53 364

54
55 365

56
57 366

58
59 367

60

References

- [1] Miceli JF, Parameswaran P, Kang DW, et al (2012) Enrichment and analysis of anode-respiring bacteria from diverse anaerobic inocula. *Environmental Science and Technology* 46:10349–10355 . doi: 10.1021/es301902h
- [2] Singh HM, Pathak AK, Chopra K, et al (2018) Microbial fuel cells: a sustainable solution for bioelectricity generation and wastewater treatment. *Biofuels* 7269:1–21 . doi: 10.1080/17597269.2017.1413860
- [3] Saratale GD, Saratale RG, Shahid MK, et al (2017) A comprehensive overview on electro-active biofilms, role of exo-electrogens and their microbial niches in microbial fuel cells (MFCs). *Chemosphere* 178:534–547 . doi: 10.1016/j.chemosphere.2017.03.066
- [4] Aguirre-Sierra A, Bacchetti-De Gregoris T, Berná A, et al (2016) Microbial electrochemical systems outperform fixed-bed biofilters in cleaning up urban wastewater. *Environ Sci: Water Res Technol* 2:984–993 . doi: 10.1039/C6EW00172F
- [5] Pierra M, Carmona-Martínez AA, Trably E, et al (2015) Microbial characterization of anode-respiring bacteria within biofilms developed from cultures previously enriched in dissimilatory metal-reducing bacteria. *Bioresource Technology* 195:283–287 . doi: 10.1016/j.biortech.2015.07.010
- [6] Doyle LE, Marsili E (2015) Methods for enrichment of novel electrochemically-active microorganisms. *Bioresource Technology* 195:273–282 . doi: 10.1016/j.biortech.2015.07.025
- [7] Koch C, Harnisch F (2016) Is there a Specific Ecological Niche for Electroactive Microorganisms? *ChemElectroChem* 3:1282–1295 . doi: 10.1002/celc.201600079
- [8] Zhang YC, Jiang ZH, Liu Y (2015) Application of electrochemically active bacteria as anodic biocatalyst in microbial fuel cells. *Chinese Journal of Analytical Chemistry* 43:155–163 . doi: 10.1016/S1872-2040(15)60800-3
- [9] Kubota K, Watanabe T, Yamaguchi T, Syutsubo K (2016) Characterization of wastewater treatment by two microbial fuel cells in continuous flow operation. *Environmental Technology* 37:114–120 . doi: 10.1080/09593330.2015.1064169
- [10] Haavisto JM, Lakaniemi AM, Puhakka JA (2018) Storing of exoelectrogenic anolyte for efficient microbial fuel cell recovery. *Environmental Technology* 1–9 . doi: 10.1080/09593330.2017.1423395

- [11] Zhang Y, Zhao Y-G, Guo L, Gao M (2018) Two-stage pretreatment of excess sludge for electricity generation in microbial fuel cell. *Environmental Technology* 1–10 . doi: 10.1080/09593330.2017.1422548
- [12] Sleutels THJA, Darus L, Hamelers HVM, Buisman CJN (2011) Effect of operational parameters on Coulombic efficiency in bioelectrochemical systems. *Bioresource Technology* 102:11172–11176 . doi: 10.1016/j.biortech.2011.09.078
- [13] Liu Y, Harnisch F, Fricke K, et al (2008) Improvement of the anodic bioelectrocatalytic activity of mixed culture biofilms by a simple consecutive electrochemical selection procedure. *Biosensors and Bioelectronics* 24:1006–1011 . doi: 10.1016/j.bios.2008.08.001
- [14] Kim JR, Min B, Logan BE (2005) Evaluation of procedures to acclimate a microbial fuel cell for electricity production. *Applied Microbiology and Biotechnology* 68:23–30 . doi: 10.1007/s00253-004-1845-6
- [15] Sathish-Kumar K, Solorza-Feria O, Tapia-Ramírez J, et al (2013) Electrochemical and chemical enrichment methods of a sodic–saline inoculum for microbial fuel cells. *International Journal of Hydrogen Energy* 38:12600–12609 . doi: 10.1016/J.IJHYDENE.2012.11.147
- [16] Wang A, Sun D, Ren N, et al (2010) A rapid selection strategy for an anodophilic consortium for microbial fuel cells. *Bioresource Technology* 101:5733–5735 . doi: 10.1016/j.biortech.2010.02.056
- [17] Torres CI, Krajmalnik-Brown R, Parameswaran P, et al (2009) Selecting Anode-Respiring Bacteria Based on Anode Potential: Phylogenetic, Electrochemical, and Microscopic Characterization. *Environmental Science and Technology* 43:9519–9524 . doi: 10.1021/es902165y
- [18] Stratford JP, Beecroft NJ, Slade RCT, et al (2014) Anodic microbial community diversity as a predictor of the power output of microbial fuel cells. *Bioresource Technology* 156:84–91 . doi: 10.1016/j.biortech.2014.01.041
- [19] Yamamoto S, Suzuki K, Araki Y, et al (2014) Dynamics of Different Bacterial Communities Are Capable of Generating Sustainable Electricity from Microbial Fuel Cells with Organic Waste. *Microbes Environ* 29:145–153 . doi: 10.1264/jsme2.ME13140
- [20] Agostino V, Ahmed D, Sacco A, et al (2017) Electrochemical analysis of microbial fuel cells based on enriched biofilm communities from freshwater sediment. *Electrochimica Acta* 237:133–

- 428 143 . doi: 10.1016/j.electacta.2017.03.186
- 429 [21] Zhi W, Ge Z, He Z, Zhang H (2014) Methods for Understanding Microbial Community
430 Structures and Functions in Microbial Fuel Cells : a Review. *Bioresource Technology* 171:461–
431 468 . doi: 10.1016/j.biortech.2014.08.096
- 432 [22] Schilirò T, Tommasi T, Armato C, et al (2016) The study of electrochemically active planktonic
433 microbes in microbial fuel cells in relation to different carbon-based anode materials. *Energy*
434 106:277–284 . doi: 10.1016/j.energy.2016.03.004
- 435 [23] Muyzer G, De Waal EC, Uitterlinden AG (1993) Profiling of complex microbial populations by
436 denaturing gradient gel electrophoresis analysis of polymerase chain reaction-amplified genes
437 coding for 16S rRNA. *Applied and Environmental Microbiology* 59:695–700 . doi: 0099-
438 2240/93/030695-06\$02.00/0
- 439 [24] Webster G, Parkes RJ, Cragg BA, et al (2006) Prokaryotic community composition and
440 biogeochemical processes in deep seafloor sediments from the Peru Margin. *FEMS*
441 *Microbiology Ecology* 58:65–85 . doi: 10.1111/j.1574-6941.2006.00144.x
- 442 [25] O’Sullivan LA, Webster G, Fry JC, et al (2008) Modified linker-PCR primers facilitate complete
443 sequencing of DGGE DNA fragments. *Journal of Microbiological Methods* 75:579–581 . doi:
444 10.1016/j.mimet.2008.08.006
- 445 [26] Murri M, Leiva I, Gomez-Zumaquero JM, et al (2013) Gut microbiota in children with type 1
446 diabetes differs from that in healthy children: a case-control study. *BMC Med* 11:46 . doi:
447 10.1186/1741-7015-11-46
- 448 [27] Yang YW, Chen MK, Yang BY, et al (2015) Use of 16S rRNA gene-targeted group-specific
449 primers for real-time PCR analysis of predominant bacteria in mouse feces. *Applied and*
450 *Environmental Microbiology* 81:6749–6756 . doi: 10.1128/AEM.01906-15
- 451 [28] Bacchetti De Gregoris T, Aldred N, Clare AS, Burgess JG (2011) Improvement of phylum- and
452 class-specific primers for real-time PCR quantification of bacterial taxa. *Journal of*
453 *Microbiological Methods* 86:351–356 . doi: 10.1016/j.mimet.2011.06.010
- 454 [29] Hermann-Bank ML, Skovgaard K, Stockmarr A, et al (2013) The Gut Microbiotassay: a high-
455 throughput qPCR approach combinable with next generation sequencing to study gut microbial
456 diversity. *BMC genomics* 14:788 . doi: 10.1186/1471-2164-14-788
- 457 [30] Cummings DE, Snoeyenbos-West OL, Newby DT, et al (2003) Diversity of Geobacteraceae

- species inhabiting metal-polluted freshwater lake sediments ascertained by 16S rDNA analyses. Microbial Ecology 46:257–269 . doi: 10.1007/s00248-002-0005-8
- [31] de Souza JT, Mazzola M, Raaijmakers JM (2003) Conservation of the response regulator gene *gacA* in *Pseudomonas* species. Environ Microbiol 5:1328–1340 . doi: 10.1046/j.1462-2920.2003.00438.x
- [32] Dridi B, Henry M, El Khéchine A, et al (2009) High prevalence of *Methanobrevibacter smithii* and *Methanosphaera stadtmanae* detected in the human gut using an improved DNA detection protocol. PLoS ONE 4: . doi: 10.1371/journal.pone.0007063
- [33] Carriço JA, Pinto FR, Simas C, et al (2005) Assessment of band-based similarity coefficients for automatic type and subtype classification of microbial isolates analyzed by pulsed-field gel electrophoresis. Journal of Clinical Microbiology 43:5483–5490 . doi: 10.1128/JCM.43.11.5483-5490.2005
- [34] Cristiani P, Franzetti A, Gandolfi I, et al (2013) Bacterial DGGE fingerprints of biofilms on electrodes of membraneless microbial fuel cells. International Biodeterioration and Biodegradation 84:211–219 . doi: 10.1016/j.ibiod.2012.05.040
- [35] Beecroft NJ, Zhao F, Varcoe JR, et al (2012) Dynamic changes in the microbial community composition in microbial fuel cells fed with sucrose. Applied Microbiology and Biotechnology 93:423–437 . doi: 10.1007/s00253-011-3590-y
- [36] Kim JR, Beecroft NJ, Varcoe JR, et al (2011) Spatiotemporal development of the bacterial community in a tubular longitudinal microbial fuel cell. Applied Microbiology and Biotechnology 90:1179–1191 . doi: 10.1007/s00253-011-3181-y
- [37] Sun G, Thygesen A, Meyer AS (2015) Acetate is a superior substrate for microbial fuel cell initiation preceding bioethanol effluent utilization. Applied Microbiology and Biotechnology 99:4905–4915 . doi: 10.1007/s00253-015-6513-5
- [38] Sotres A, Díaz-Marcos J, Guivernau M, et al (2015) Microbial community dynamics in two-chambered microbial fuel cells: effect of different ion exchange membranes. Journal of Chemical Technology & Biotechnology 90:1497–1506 . doi: 10.1002/jctb.4465
- [39] Stewart EJ (2012) Growing unculturable bacteria. Journal of Bacteriology 194:4151–4160 . doi: 10.1128/JB.00345-12
- [40] Chae KJ, Choi MJ, Lee JW, et al (2009) Effect of different substrates on the performance,

- 488 bacterial diversity, and bacterial viability in microbial fuel cells. *Bioresource Technology*
489 100:3518–3525 . doi: 10.1016/j.biortech.2009.02.065
- 490 [41] Liu Q, Yang Y, Mei X, et al (2018) Response of the microbial community structure of biofilms to
491 ferric iron in microbial fuel cells. *Science of the Total Environment* 631–632:695–701 . doi:
492 10.1016/j.scitotenv.2018.03.008
- 493 [42] Sotres A, Cerrillo M, Viñas M, Bonmatí A (2015) Nitrogen recovery from pig slurry in a two-
494 chambered bioelectrochemical system. *Bioresource Technology* 194:373–382 . doi:
495 10.1016/j.biortech.2015.07.036
- 496 [43] Sotres A, Tey L, Bonmatí A, Viñas M (2016) Microbial community dynamics in continuous
497 microbial fuel cells fed with synthetic wastewater and pig slurry. *Bioelectrochemistry* 111:70–82
498 . doi: 10.1016/j.bioelechem.2016.04.007
- 499 [44] Bonmatí A, Sotres A, Mu Y, et al (2013) Oxalate degradation in a bioelectrochemical system:
500 Reactor performance and microbial community characterization. *Bioresource Technology*
501 143:147–153 . doi: 10.1016/j.biortech.2013.05.116
- 502 [45] Kannaiah Goud R, Venkata Mohan S (2013) Prolonged applied potential to anode facilitate
503 selective enrichment of bio-electrochemically active Proteobacteria for mediating electron
504 transfer: Microbial dynamics and bio-catalytic analysis. *Bioresource Technology* 137:160–170 .
505 doi: 10.1016/j.biortech.2013.03.059
- 506 [46] Hu A, Yang X, Chen N, et al (2014) Response of bacterial communities to environmental
507 changes in a mesoscale subtropical watershed, Southeast China. *Science of the Total*
508 *Environment* 472:746–756 . doi: 10.1016/j.scitotenv.2013.11.097
- 509 [47] Rago L, Baeza JA, Guisasola A (2016) Increased performance of hydrogen production in
510 microbial electrolysis cells under alkaline conditions. *Bioelectrochemistry* 109:57–62 . doi:
511 10.1016/j.bioelechem.2016.01.003
- 512 [48] Margaria V, Tommasi T, Pentassuglia S, et al (2017) Effects of pH variations on anodic marine
513 consortia in a dual chamber microbial fuel cell. *International Journal of Hydrogen Energy*
514 42:1820–1829 . doi: 10.1016/j.ijhydene.2016.07.250
- 515 [49] Wang Z, Lee T, Lim B, et al (2014) Microbial community structures differentiated in a single-
516 chamber air-cathode microbial fuel cell fueled with rice straw hydrolysate. *Biotechnology for*
517 *Biofuels* 7:9 . doi: 10.1186/1754-6834-7-9

1
2
3 518 [50] Rago L, Ruiz Y, Baeza JA, et al (2015) Microbial community analysis in a long-term membrane-
4
5 519 less microbial electrolysis cell with hydrogen and methane production. *Bioelectrochemistry*
6
7 520 106:359–368 . doi: 10.1016/j.bioelechem.2015.06.003
8
9 521 [51] Lee Y-Y, Kim TG, Cho K (2015) Effects of proton exchange membrane on the performance and
10
11 522 microbial community composition of air-cathode microbial fuel cells. *Journal of Biotechnology*
12
13 523 211:130–137 . doi: 10.1016/j.jbiotec.2015.07.018
14
15 524 [52] Spiegelman D, Whissell G, Greer CW (2005) A survey of the methods for the characterization of
16
17 525 microbial consortia and communities. *Canadian Journal of Microbiology* 51:355–386 . doi:
18
19 526 10.1139/w05-003
20
21 527 [53] Rittmann BE, Krajmalnik-Brown R, Halden RU (2008) Pre-genomic, genomic and post-genomic
22
23 528 study of microbial communities involved in bioenergy. *Nature Reviews Microbiology* 6:604–612
24
25 529 . doi: 10.1038/nrmicro1939
26
27 530 [54] Harnisch F, Rabaey K (2012) The diversity of techniques to study electrochemically active
28
29 531 biofilms highlights the need for standardization. *ChemSusChem* 5:1027–1038 . doi:
30
31 532 10.1002/cssc.201100817
32
33 533
34 534
35 535
36
37 536
38
39 537
40
41 538
42
43 539
44
45 540
46
47 541
48
49 542
50
51 543
52
53 544
54
55
56 545
57
58 546
59
60

547 **Tables**

548 Table 1. Targets, primers, amplicon size, annealing temperature and genomic standards used in real time

549 qPCR. Ta= annealing temperature, bp= base pair.

Target	Primers	Amplicon size (bp); Ta	Standard	Reference
Bacteroidetes	F CATGTGGTTTAATTCGATGAT R AGCTGACGACAACCATGCAG	126 Ta: 60°C	<i>Bacteroides fragilis</i>	[26]
β-Proteobacteria	Beta979F AACGCGAAAAACCTTACCTACC Beta1130R TGCCCTTTCGTAGCAACTAGTG	174 Ta: 50°C	<i>Alcaligenes faecalis</i>	[27]
γ-Proteobacteria	1080yF TCGTCAGCTCGTGTGTGA Y1202R CGTAAGGGCCATGATG	170 Ta: 52°C	<i>Shewanella oneidensis</i>	[28]
δ-Proteobacteria	F: GGTGTAGGAGTGAARTCCGT R: TACGTGTGTAGCCCTRGRC	534 Ta: 55°C	<i>Geobacter metallireducens</i>	[29]
Firmicutes	F: ATGTGGTTTAATTCGAAGCA R: AGCTGACGACAACCATGCAC	126 Ta: 60 °C	<i>Clostridium difficile</i>	[26]
Geobacteraceae spp.	Geo564F AAGCGTTGTTCCGAWTTAT Geo840R GGCACTGCAGGGGTCAATA	277 Ta: 55°C	<i>Geobacter metallireducens</i>	[30]
Pseudomonas spp.	gacA1 GBATCGGMGGYCTBGARGC gacA2 MGYCARYTCVACRTCRCCTGSTGAT	425 Ta: 61°C	<i>Pseudomonas aeruginosa</i>	[31]
Total Bacteria	16S RNA F AGAGTTTGATCMTGGCTCAG 16S RNA R TTACCGCGGCKGCTGGCAC Probe CCAKACTCCTACGGGAGGCAGCAG	About 600 Ta: 55°C	<i>Desulfovibrio vulgaris</i>	[32]

1
2
3
4
5
6
7
8
9
10
11
12
13
14
15
16
17
18
19
20
21
22
23
24
25
26
27
28
29
30
31
32
33
34
35
36
37
38
39
40
41
42
43
44
45
46
47
48
49
50
51
52
53
54
55
56
57
58
59
60

551 Table 2. Thermal protocol of qPCR for all strains under study. Each reaction is 40 cycles long. In the last
552 row are the Efficiency (Eff) and R² obtained from each standard curve.

Target	Total bacteria	β-Proteobacteria	γ-Proteobacteria	δ-Proteobacteria	Bacteroidetes	Firmicutes	<i>Geobacteriaceae</i> spp.	<i>Pseudomonas</i> spp.
Initial denaturation	95°C for 3 min	95°C for 2 min	95°C for 3 min	95°C for 3 min	95°C for 2.5 min	95°C for 2.5 min	95°C for 3 min	95°C for 2.5 min
Denaturation	95°C for 30 s	95°C for 10 s	95°C for 30 s	95°C for 30 s	95°C for 10 s	95°C for 10 s	95°C for 30 s	95°C for 30 s
Annealing	55°C for 30 s	50°C for 30 s	52°C for 30 s	55°C for 30 s	60°C for 20 s	60°C for 20 s	55°C for 30 s	61°C for 30 s
Extension	72°C for 30 s		72°C for 30 s	72°C for 36 s	72°C for 15 s	72°C for 15 s	72°C for 30 s	72°C for 36 s
	–	Melt curve	Melt curve	Melt curve	Melt curve	Melt curve	Melt curve	Melt curve
Standard curve parameters	Eff= 90.8 R ² =0.992	Eff= 99.9 R ² =0.999	Eff= 95.3 R ² =0.991	Eff= 95.4 R ² =0.998	Eff= 97.1 R ² =0.999	Eff= 100.7 R ² =0.999	Eff= 104.0 R ² =0.998	Eff= 99.7 R ² =0.999

553
554
555
556
557
558
559
560
561
562
563

Table 3. Sequencing analysis of the band excised from DGGE lanes of inoculum and first and third preculture enrichment steps. Accession number and percentage of similarity are also reported.

Band	Closest relative	Phylum	Class	accession n°	Similarity %
1	Uncultured γ -proteobacterium	Proteobacteria	γ -proteobacteria	HE856452	95
2	<i>Acinetobacter sp.</i>	Proteobacteria	γ -proteobacteria	JN082732	98
3	Uncultured β -proteobacterium	Proteobacteria	β -proteobacteria	KC602997	86
4	<i>Alcaligenes sp.</i>	Proteobacteria	β -proteobacteria	KX345927	93
5	<i>Acinetobacter sp.</i>	Proteobacteria	γ -proteobacteria	KP943116	100
6	Bacterium enrichment culture		nd	FJ842606	98
7	<i>Arcobacter sp.</i>	Proteobacteria	ϵ -proteobacteria	KP182157	99
8	Uncultured <i>Trichococcus sp.</i>	Firmicutes	Bacilli	KR911832	99
9	Uncultured bacterium		nd	LN651052	96
10	Uncultured bacterium		nd	KU362745	99
11	Uncultured <i>Clostridium sp.</i>	Firmicutes	Clostridia	KU764678	99
12	<i>Trichococcus sp.</i>	Firmicutes	Bacilli	KT424954	93
13	<i>Bacillus sp.</i>	Firmicutes	Bacilli	KJ743291	100
14	Uncultured <i>Agrobacterium sp.</i>	Proteobacteria	α -proteobacteria	JN625545	100
15	Uncultured <i>Comamonas sp.</i>	Proteobacteria	β -proteobacteria	KX010337	100
16	<i>Rhizobium sp.</i>	Proteobacteria	α -proteobacteria	KC252885	99
17	Uncultured <i>Geobacter sp.</i>	Proteobacteria	δ -proteobacteria	LC001501	99
18	Uncultured <i>Clostridiales sp.</i>	Firmicutes	Clostridia	KJ185096	100

1
2
3
4
5
6
7
8
9
10
11
12
13
14
15
16
17
18
19
20
21
22
23
24
25
26
27
28
29
30
31
32
33
34
35
36
37
38
39
40
41
42
43
44
45
46
47
48
49
50
51
52
53
54
55
56
57
58
59
60

Table 4. Sequencing analysis of the band excised from DGGE lanes of planktonic, carbon felt biofilm and graphite rod components at the end of the test. Accession number and percentage of similarity are reported.

Band	Closest relative	Phylum	Class	accession n°	Similarity %
1	<i>Comamonas sp.</i>	Proteobacteria	β -proteobacteria	KX225279	98
2	<i>Pseudomonas sp.</i>	Proteobacteria	γ -proteobacteria	AY954288	98
3	Uncultured <i>Alcaligenes sp.</i>	Proteobacteria	β -proteobacteria	LC001185	99
4	Uncultured β -proteobacteria	Proteobacteria	β -proteobacteria	CU920026	91
5	Uncultured <i>Comamonas sp.</i>	Proteobacteria	β -proteobacteria	AB793337	100
6	<i>Comamonas sp.</i>	Proteobacteria	β -proteobacteria	KX225279	100
7	<i>Rhizobium sp.</i>	Proteobacteria	α -proteobacteria	JN688942	99
8	Uncultured <i>Arcobacter sp.</i>	Proteobacteria	ϵ -proteobacteria	JX944559	99
9	Uncultured <i>Alcaligenes sp.</i>	Proteobacteria	β -proteobacteria	LC001185	99
10	Uncultured <i>Alcaligenes sp.</i>	Proteobacteria	β -proteobacteria	LC001185	100
11	<i>Arcobacter sp.</i>	Proteobacteria	ϵ -proteobacteria	FJ968638	99
12	Uncultured bacterium		nd	LN651026	83
13	<i>Pseudomonas sp.</i>	Proteobacteria	γ -proteobacteria	LN885540	99
14	<i>Arcobacter sp.</i>	Proteobacteria	ϵ -proteobacteria	FJ968638	99
15	<i>Comamonas sp.</i>	Proteobacteria	β -proteobacteria	KX225279	100
16	Uncultured <i>Geobacter sp.</i>	Proteobacteria	δ -proteobacteria	JX944527	98
17	<i>Acinetobacter sp.</i>	Proteobacteria	γ -proteobacteria	KP943121	99
18	Bacterium		nd	AJ630288	100
19	<i>Comamonas sp.</i>	Proteobacteria	β -proteobacteria	KC622039	96
20	Uncultured <i>Achromobacter sp.</i>	Proteobacteria	β -proteobacteria	LC070644	98
21	Uncultured <i>Microvirgula sp.</i>	Proteobacteria	β -proteobacteria	LC070638	99
22	<i>Comamonas sp.</i>	Proteobacteria	β -proteobacteria	KX225279	100
23	Uncultured γ -proteobacterium	Proteobacteria	γ -proteobacteria	AJ871053	89
24	<i>Comamonas sp.</i>	Proteobacteria	β -proteobacteria	KM083034	100
25	<i>Comamonas sp.</i>	Proteobacteria	β -proteobacteria	KX225279	99
26	<i>Rhizobium sp.</i>	Proteobacteria	α -proteobacteria	JN688942	99

Figure legends

Figure 1. a) DGGE profile and cluster analysis of bacterial community profile of freshwater sediment (I) and the first and third precultures (Gen = green; FeC = red). The trees were generated using Jaccard similarity. b) Shannon Index in the inoculum, Gen and FeC first (Pre1) and third (Pre3) precultures (green and red, respectively).

Figure 2. Graphical representation of relative abundance of real time qPCR products in the inoculum (top) and during the first and third preculture steps of General and FeC enrichment (bottom left and bottom right, respectively). 1° and 3° refer to the first and third step of precultures, respectively.

Figure 3. Histograms of *Geobacteraceae* spp. and *Pseudomonas* spp. real time quantification in the inoculum and during the first (Pre1) and third (Pre3) enrichment steps for the general (Gen) and ferric citrate (FeC) precultures. *Geobacteraceae* spp.: Inoculum vs FeC enrichment steps $p < 0.001$ (ANOVA, Tukey's post hoc). Inoculum vs third Gen enrichment step $p > 0.05$ (ANOVA, Tukey's post hoc). *Pseudomonas* spp. inoculum vs both third enrichment steps $p < 0.001$ (ANOVA, Tukey's post hoc).

Figure 4. a) Cluster analysis of bacterial community profile of anodic plankton (P), biofilm (B) and rod (R) of the Gen-MFC (green) and FeC-MFC (orange). The trees were generated using Jaccard similarity. b) Shannon Index at the end of test in the three different component of MFC anode (P = plankton; B = biofilm; R = rod). Gen-MFC in green and FeC-MFC in red.

Figure 5. Graphical representation of relative abundance of real time qPCR products in the planktonic (P) and attached (B+R) components at the end of the test in the general (Gen) and ferric citrate (FeC) MFCs.

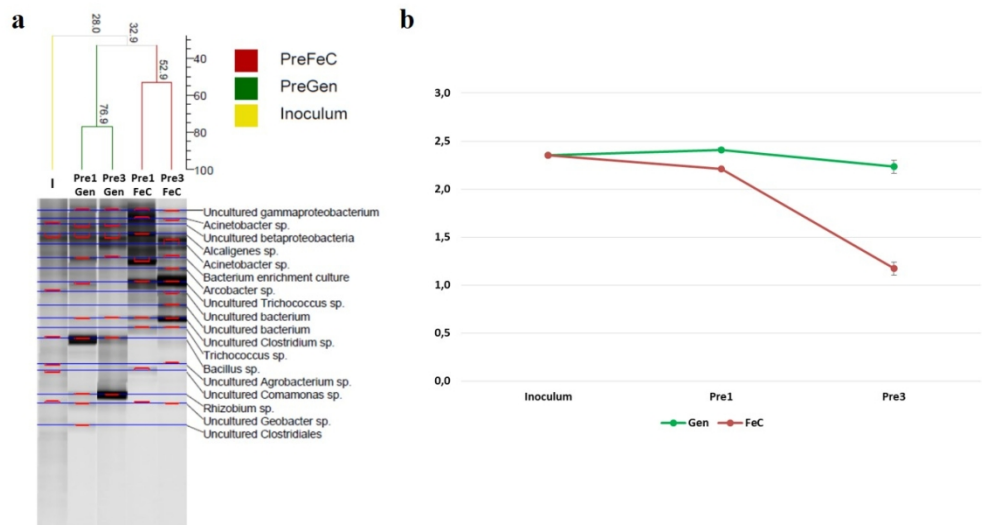


Figure 1. a) DGGE profile and cluster analysis of bacterial community profile of freshwater sediment (I) and the first and third precultures (Gen = green; FeC = red). The trees were generated using Jaccard similarity. b) Shannon Index in the inoculum, Gen and FeC first (Pre1) and third (Pre3) precultures (green and red, respectively).

114x60mm (300 x 300 DPI)

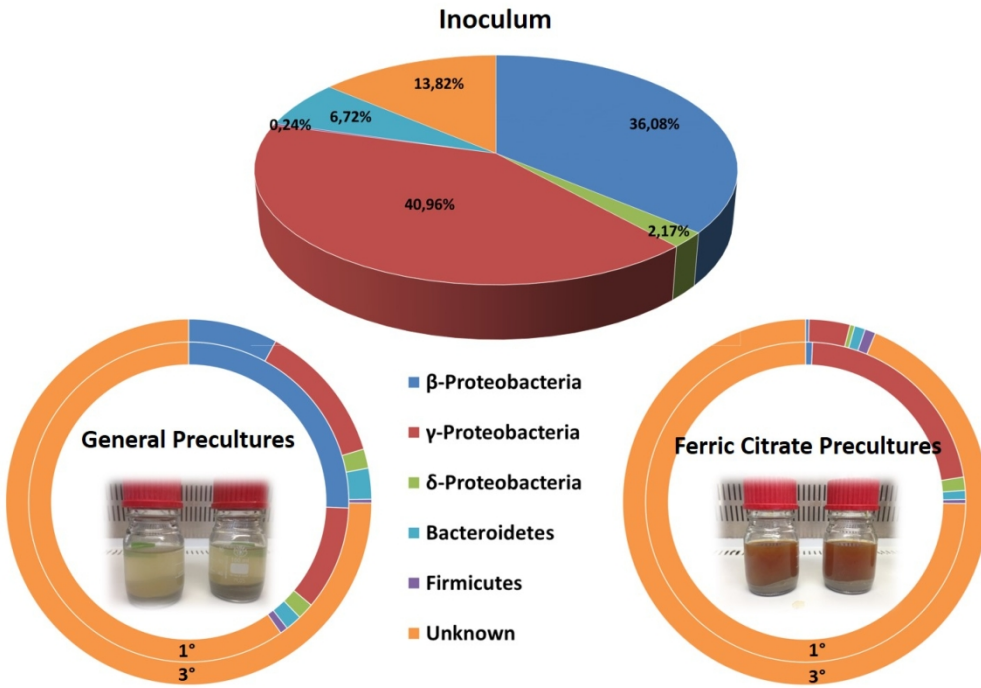


Figure 2. Graphical representation of relative abundance of real time qPCR products in the inoculum (top) and during the first and third preculture steps of General and FeC enrichment (bottom left and bottom right, respectively). 1^o and 3^o refer to the first and third step of precultures, respectively.

121x86mm (300 x 300 DPI)

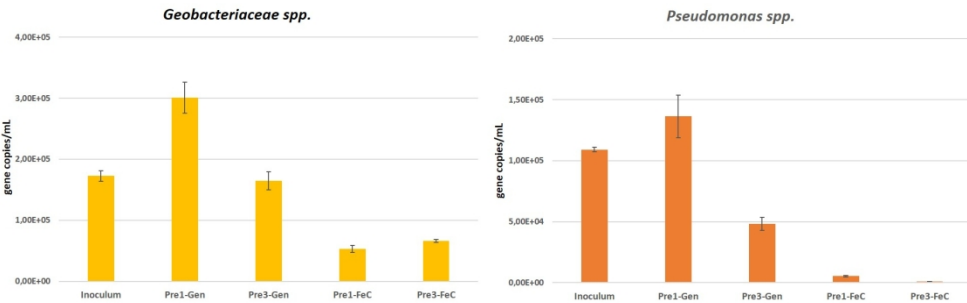


Figure 3. Histograms of *Geobacteriaceae* spp. and *Pseudomonas* spp. real time quantification in the inoculum and during the first (Pre1) and third (Pre3) enrichment steps for the general (Gen) and ferric citrate (FeC) precultures. *Geobacteriaceae* spp.: Inoculum vs FeC enrichment steps $p < 0.001$ (ANOVA, Tukey's post hoc). Inoculum vs third Gen enrichment step $p > 0.05$ (ANOVA, Tukey's post hoc). *Pseudomonas* spp. inoculum vs both third enrichment steps $p < 0.001$ (ANOVA, Tukey's post hoc).

169x52mm (300 x 300 DPI)

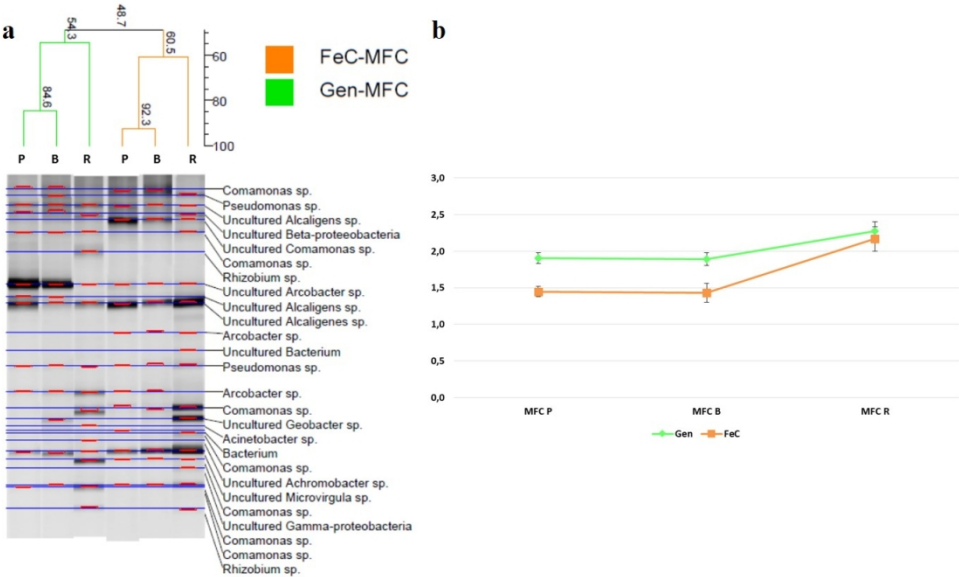


Figure 4. a) Cluster analysis of bacterial community profile of anodic plankton (P), biofilm (B) and rod (R) of the Gen-MFC (green) and FeC-MFC (orange). The trees were generated using Jaccard similarity. b) Shannon Index at the end of test in the three different component of MFC anode (P = plankton; B = biofilm; R = rod). Gen-MFC in green and FeC-MFC in red.

120x71mm (300 x 300 DPI)

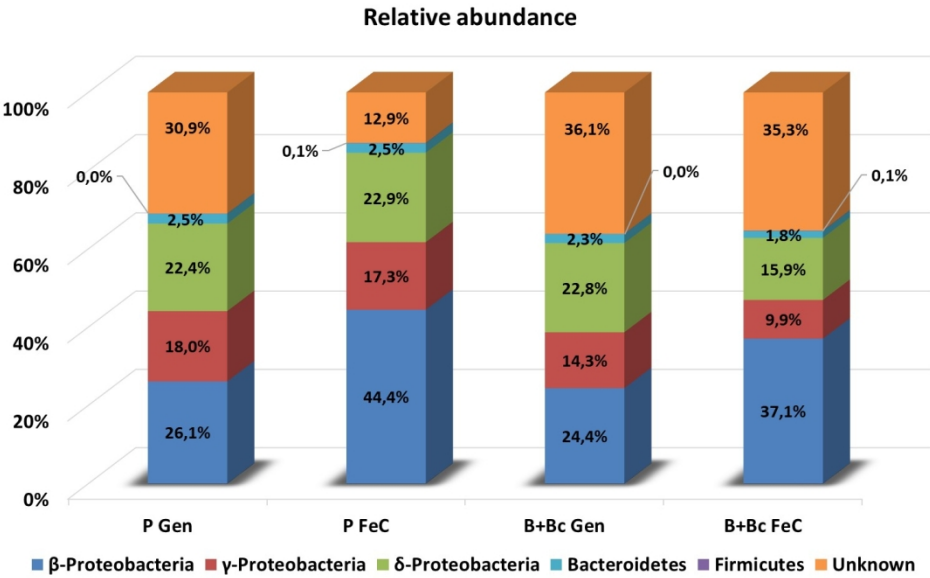
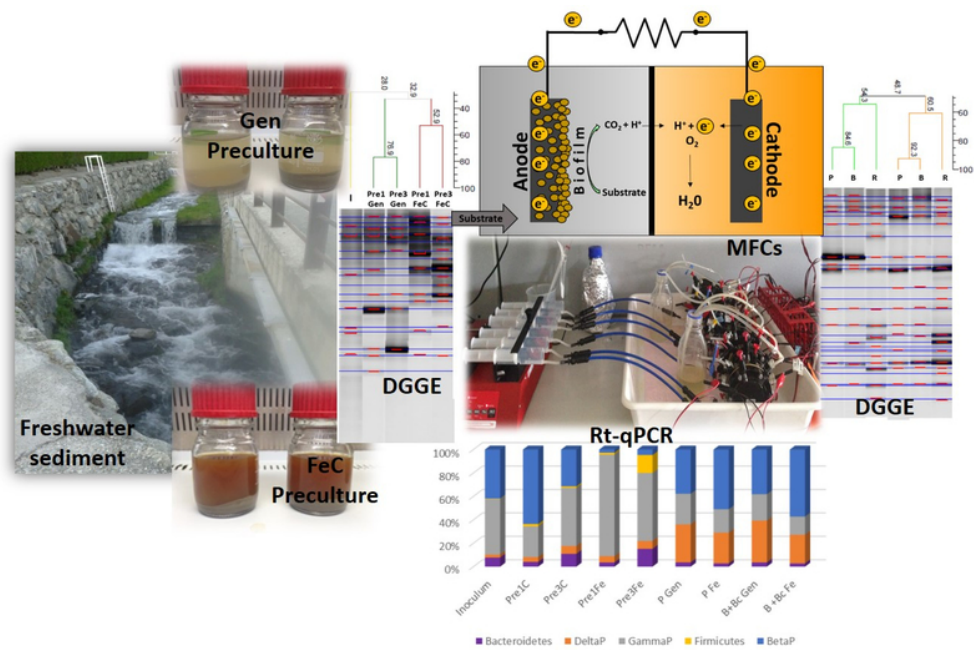


Figure 5. Graphical representation of relative abundance of real time qPCR products in the planktonic (P) and attached (B+R) components at the end of the test in the general (Gen) and ferric citrate (FeC) MFCs.

135x81mm (300 x 300 DPI)



TOC/Graphical Abstract

67x44mm (300 x 300 DPI)